Atomic- and electronic-structure study on the layers of $4Hb$-TaS_2 prepared by a layer-by-layer etching technique

Ju-Jin Kim and H. Olin
Department of Physics, Chalmers University of Technology, and Gothenburg University, S-41296, Gothenburg, Sweden
(Received 19 July 1995)

We have studied the atomic and electronic structures of $4Hb$-TaS_2, which has alternating layers of the $1T$ and $1H$ type, at room temperature and 77 K, using a scanning tunneling microscope. Using a layer-by-layer etching technique, we fabricated staircases with alternating layers of the $1T$ and $1H$ type. The T-type layers showed the typical $\sqrt{13}\times\sqrt{13}$ charge-density-wave structures, whereas the H-type layers had the triangular atomic structure at both temperatures. The measured tunneling spectra of each layer at 77 K showed entirely different characteristics; the $1H$ layer remained in the metallic state, whereas the $1T$ layer showed an insulating behavior with a wide opening of the energy gap at the Fermi level at 77 K.

Among the transition-metal dichalcogenides, the poly-type $4Hb$-TaS_2 and $4Hb$-$TaSe_2$ show interesting atomic and electronic properties, which are believed to mainly originate from the alternating layers of the trigonal prismatic coordination ($1H$) and octahedral coordination ($1T$).[1,2] These properties reflect the composite nature of those observed in the pure octahedral phases such as $1T$-TaS_2, $1T$-$TaSe_2$ and the trigonal prismatic phases such as the $2H$-TaS_2, $2H$-$TaSe_2$. Theoretical calculations and experimental results[2–4] show that each layer maintains its characteristic features found in the corresponding pure phases, although there has been a small electron transfer between the two different layers.

Particularly, the scanning tunneling microscope (STM) studies by Giambattista *et al.*[5] and Coleman *et al.*[2] showed two completely different kinds of images, one kind with a $\sqrt{13}\times\sqrt{13}$ charge-density wave (CDW) and another kind with atomic structures, on the two opposite faces of the same crystal cleave, presumably representing the $1T$-type and $1H$-type layers. They also showed a mixing of the two images and sometimes a time-dependent change of the image, which might be due to the complex superposition of two images.[2,6] Recently, Han *et al.*[7] observed strong bias-dependent STM images at room temperature. At relatively high positive bias voltage, a fully developed CDW modulation was observed even on the presumably $1H$ surface, which was explained in terms of an energy-dependent tunneling process between $1T$ and $1H$ layers. Therefore, it is very important to identify each layer precisely, that is, whether the top layer is $1T$ or $1H$. Tanaka and co-workers[8,9] tried to distinguish $1T$ from $1H$ layers using tunneling spectroscopy and obtained characteristic spectra corresponding to the $1H$- and $1T$-type layers at room temperature. However, the observed tunneling spectra at room temperature are rather obscure due to large thermal fluctuations and an interlayer tunneling effect between the neighboring layers, making it difficult to distinguish each layer precisely.

Layer-by-layer etching of the surface of transition-metal dichalcogenides has been used earlier using STM (Refs. 10 and 11) and atomic force microscope.[12] Due to the weak van der Waals force between each layer, it is possible to etch away individual layers in a well-defined manner. Using this technique, it should be possible to choose each layer in the poly-type transition-metal dichalcogenides by making successive layer-by-layer removal.

In this study, we have etched a staircase of several layers of $4Hb$-TaS_2 by a layer-by-layer etching technique and investigated the electronic and atomic structures on the newly etched region at room temperature and 77 K. The method allows us to clearly distinguish between the two types of layers that exist. The measured STM images and tunneling spectra showed the alternating nature of the $1T$- and $1H$-type layers. The $1T$-type layers showed the typical $\sqrt{13}\times\sqrt{13}$ CDW structures, whereas the $1H$-type layers had triangular atomic structure with a weakly superposed CDW superlattice at relatively high bias voltage. The measured tunneling spectra on each layer at 77 K showed entirely different characteristics between the two layers; the $1H$ layer remained in the metallic state, whereas the $1T$ layer showed an insulating behavior with a wide opening of an energy gap at the Fermi level at 77 K.

Single crystals of $4Hb$-TaS_2 were grown by the usual iodine transport method. The samples were cleaved at room temperature in air and set in the STM unit. For the room-temperature experiments, it was placed in the center of a doubly shielded cryostat in vacuum or in a He exchange gas environment. The STM unit was cooled very slowly to 77 K in the high vacuum state for low-temperature experiments. Mechanically polished Pt/Ir tips were used. All images were obtained in the constant current mode.

Figure 1(a) shows an STM image (1250 Å$\times$1250 Å) of the $4Hb$-TaS_2 single crystal. The tunneling current and bias voltage were 10 nA and 32 mV, respectively. The etching was performed during scanning. First, the full area was scanned while the whole etching processes were monitored by STM imaging. Small defect regions grew very slowly as the tip was scanned across the layer and suddenly, a large part of the layer was removed. After removing, we measured STM images on this specific layer but with a smaller scan area. After then, we returned to etching of the next layer with the full area scan, and so on. Continuing the scanning and measuring process (about 40-min scan) resulted in the re-

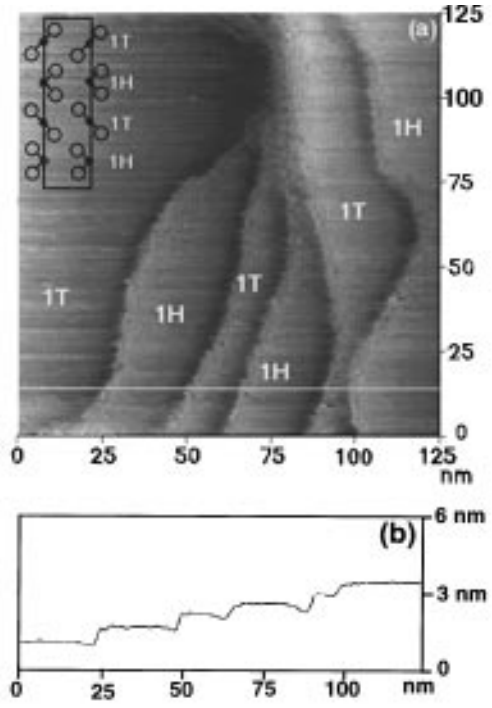

FIG. 1. (a) STM image of $4Hb$-TaS_2 after layer-by-layer etching during 40 min of continuous scanning at room temperature in constant current mode. The sample bias current and voltage were 10 nA and 32 mV, respectively. (b) The cross-sectional profile noted by the white straight line in the STM image. Inset: the schematic crystal structure of $4Hb$-TaS_2 along the 1120 section. The black and white circles represent the Ta and S atomos, respectively (Ref. 1).

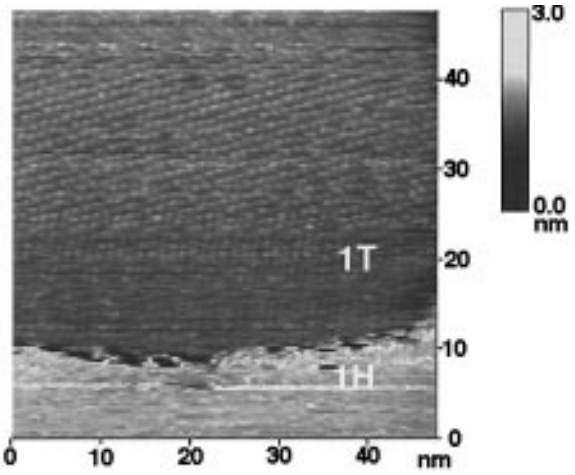

FIG. 2. STM image after one-layer etching near one of the boundary regions with one molecular step, the height of which is ≈ 6 Å. The sample bias current and voltage were 10 nA and 32 mV, respectively.

moval of several layers as shown in Fig. 1(a). We can clearly see six flat surface layers in this figure. Figure 1(b) shows the cross-sectional profile along the line indicated by the white straight line in Fig. 1(a). The step height was estimated to about 5–7 Å, which is equal to the lattice constant along the c axis in each layer within experimental error [refer to the inset of Fig. 1(a)]. It shows that every step is made up of one S-Ta-S molecular layer.

Figure 2 shows an STM image near one of the boundary regions with one molecular step (≈ 6 Å), after one layer etching. It shows clearly two regions separated by a step. The upper layer in the lower part of the figure shows a rather flat surface with no structure, whereas a strong modulation with a periodicity ≈ 12 Å is visible in the lower layer. The upper layer is most probably a $1H$-type surface as it shows an atomic structure with a lattice constant ≈ 3.3 Å. In this wide (480 Å$\times$480 Å) scan, the atomic lattice would appear as a flat surface with no structure. However, the $\sqrt{13}\times\sqrt{13}$ CDW superlattice is clearly resolved in the lower layer corresponding to the $1T$ layer.

To study the more detailed atomic structures in each layer, we also measured STM images with small scan areas $\approx 94\times 94$ Å^2 in each layer during the etching process. The STM image of the top layer in Fig. 1(a) showed a typical triangular atomic lattice with an amplitude ~ 0.4 Å as in Fig. 3(a). At relatively high positive bias voltage (about 200 mV), we also observed a weak CDW modulation believed to arise from the second $1T$ layer. This is shown in Fig. 3(b). In this case, the amplitude of the CDW modulation was relatively small and about 1.2 Å at a bias voltage of 214 mV. This is smaller than the results obtained by Han *et al.*,[7] who observed the fully developed CDW modulation both presumably in the $1T$ layer and in the $1H$ layer at a bias voltage larger than 170 mV. We believe that this discrepancy is caused by a difference in the strength of interlayer interactions, which depends on the sample quality. In the second layer, we obtained a very strong $\sqrt{13}\times\sqrt{13}$ CDW modulation about ~ 2.3 Å [Fig. 3(c)]. Subsequent measurements showed that the third layer had a triangular lattice with a small atomic corrugation ~ 0.4 Å, the fourth layer had the same strong CDW superlattice as the second layer, and so on. Thus, we could confirm the alternating structures of $1T$ and $1H$ layers in the poly-type $4Hb$-TaS_2 very clearly and directly.

We have also measured tunneling spectra for the two types of layers at room temperature and at 77 K which were prepared by the layer-by-layer etching. To avoid multiple tunnel junction effects across the barriers made up of the alternating $1T$ and $1H$ layers along the c axis, we made electrical contacts around the rim of the whole sample except the top layer in the scanning region. Otherwise, we would see the spectra from a multiple tunneling junction between the layers, particularly at low temperatures, and not the intrinsic properties of the specified layer.[6] Figures 3(a) and 3(b) show typical tunneling spectra at both temperatures on the $1T$ and $1H$ layers, respectively.

By comparing the spectra of the $1T$ layer at room temperature and at 77 K in Fig. 4(a), it is clear that the general shapes of the two tunneling spectra are quite close to each other except for the magnitude of the density of states (DOS) at the Fermi level. However, they are quite different from the spectra of the pure $1T$-TaS_2 in the nearly commensurate phase.[13–15] It may reflect the commensurate nature, i.e., the absence of the domain structure on the surface of the $1T$ layer in the $4Hb$-TaS_2. Lowering the temperature, the DOS at the Fermi level decreased appreciably and showed more of the insulating nature at 77 K. We also observed a strong depletion of the DOS at the Fermi level at 77 K with a gap

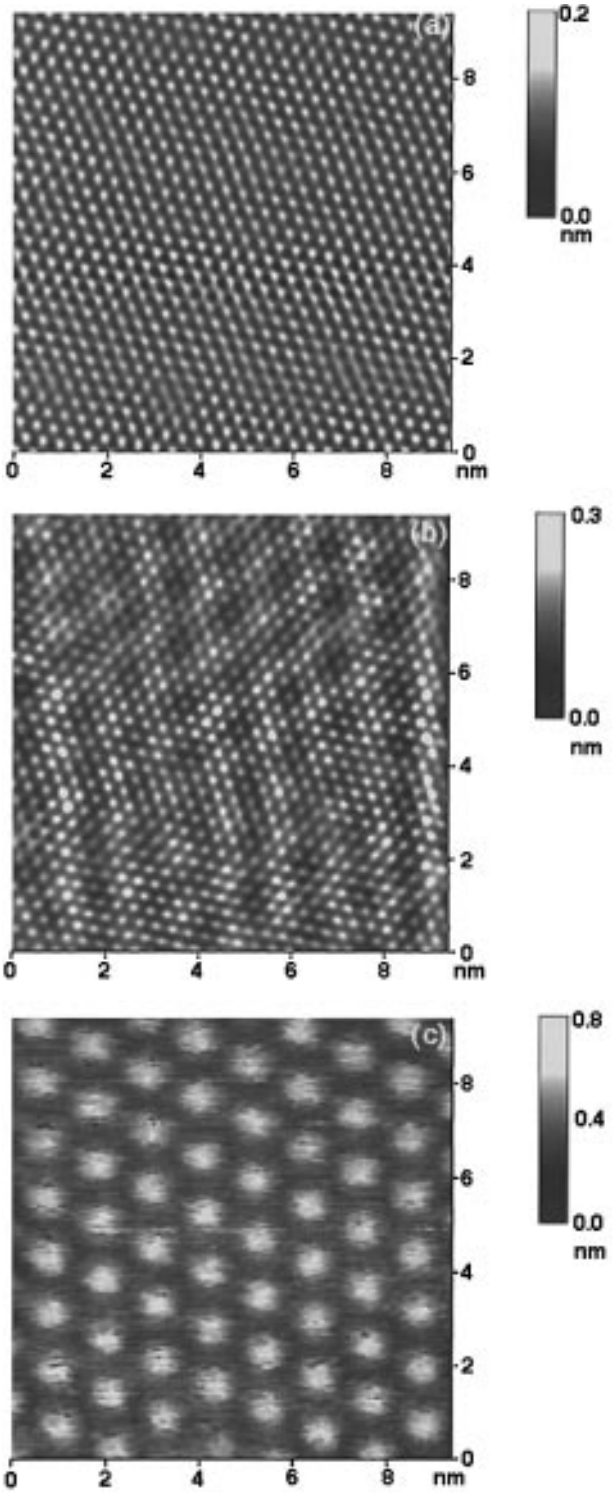

FIG. 3. (a) A typical STM image on the surface of the $1H$ layer in Fig. 1(a). The sample bias current and voltage were 10 nA and 32 mV, respectively. (b) The STM image on the same surface as in (a) with a high bias voltage (214 mV). (c) A typical STM image of the surface of the $1T$ layer in Fig. 1(a). The sample bias current and voltage were 10 nA and 32 mV, respectively.

structure at $V \approx -250$ mV, the shape of which is quite close to the tunneling[16] and the photoelectron spectroscopy (PES) measurements of the commensurate $1T$-TaS_2.[14,15] The dotted line in Fig. 4(a) shows the tunneling spectra on the next

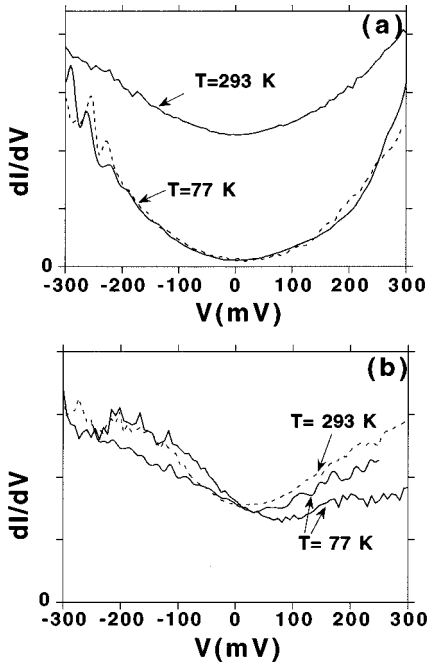

FIG. 4. (a) Tunneling spectra at 293 and 77 K measured on the $1T$ layers. (b) Tunneling spectra at 293 and 77 K measured on the $1H$ layers. The bias current and voltage were 2 nA (2 nA) and 200 mV (100 mV) on the $1T$ ($1H$) layer. The spectra were normalized at high bias voltage.

$1T$ layer, proving good reproducibility. Similar tunneling spectra were obtained reproducibly in every experiment of the $1T$ layer. Considering that the $1T$ layer in $4Hb$-TaS_2 does not experience a phase transition between room temperature and 77 K,[1,2] it is believed that the $1T$ layer in the poly-type has similar electrical properties as found in pure commensurate $1T$ phases without serious modifications. However, it is not clear whether the $1T$ layer in $4Hb$-TaS_2 would be a Mott insulator like the commensurate $1T$-TaS_2.[14–16] More systematic studies on this layer will be needed to clarify this, using other tools including temperature-dependent PES combined with band calculations.

Figure 4(b) shows the tunneling spectra of the $1H$ layer of $4Hb$-TaS_2 at both temperatures. The tunneling spectra show a relatively large finite DOS at the Fermi level at both temperatures. The $1H$ layer kept its characteristic peak structures in the tunneling spectra and remained in the metallic state at the low temperature unlike the $1T$ layer. It indicates that the metallic $1H$ layers are separated by insulating $1T$ layers. Two tunneling spectra at 77 K in Fig. 4(b), which show a somewhat different shape, were obtained at different $1H$ layers of the same sample. However, we obtained very reproducible tunneling spectra at the same position. Although the tunneling spectra on $1H$ layers of the same sample showed a little different shape as the measurement position changed, it is still in the metallic state with a finite DOS at the Fermi level at 77 K.

The resistivity measurements by Wattamaniuk, Tidman, and Frindt[17] showed that the tunneling conduction between the layers is considerable at high temperatures, due to the small activation energy (about 4 meV) required to surmount

the interlayer barriers via thermally activated hopping from layer to layer. The interlayer conduction would contribute in part to the finite DOS at the Fermi level observed in the $1T$ layer at room temperature. The large thermal fluctuations also limit the energy resolution of the spectra around the Fermi level at high temperature. Hence, it might be nontrivial to discriminate each layer at room temperature even though they have a little different shape from each other.[8,9] Lowering the temperature, the interlayer tunneling would decrease and reveal the insulating properties of the $1T$ layer itself at sufficiently low temperature. At 77 K, we can distinguish one layer from the other in terms of tunneling spectra very clearly as in Fig. 4; one layer shows the insulating behavior with a strong depletion of the DOS around the Fermi level; the other has metallic characteristics with a finite DOS at the Fermi level. It shows clearly that $4Hb$-TaS_2 can be described as a stack of alternating metallic and insulating layers. This is quite consistent with the resistivity measurement result.[17]

In summary, we have studied the atomic and electronic structures on the surfaces of $1T$ and $1H$ layers in $4Hb$-TaS_2, where the individual layers were prepared by layer-by-layer etching using STM. More than six layers have been fabricated in depth and the STM images and tunneling spectra were measured simultaneously during the etching process. STM images on each layer showed the alternating structure consisting of $1T$- and $1H$-type layers directly. The measured tunneling spectra of each layer at low temperature also revealed the stacking nature of alternating metallic and insulating layers very clearly.

This work was supported by the Swedish Research Council for Engineering Science (TFR). We would like to thank Dr. Hans Starnberg and Professor F. Levy for providing us with the single crystals.

[1] J. A. Wilson, F. J. DiSalvo, and S. Mahasan, Adv. Phys. **24**, 117 (1975).
[2] R. V. Coleman, B. Giambattista, P. K. Hansma, A. Johnson, W. W. McNairy, and C. G. Slough, Adv. Phys. **37**, 559 (1988).
[3] R. H. Friend, D. Jerome, R. F. Frind, and A. J. Yoffe, J. Phys. C **10**, 1013 (1977).
[4] N. J. Doran, G. Wexler, and A. M. Woolley, J. Phys. C **11**, 2967 (1978).
[5] B. Giambattista, A. Johnson, W. W. McNairy, C. G. Slough, and R. V. Coleman, Phys. Rev. B **38**, 3545 (1988).
[6] R. V. Coleman, Z. Dai, W. W. McNairy, C. G. Slough, and C. Wang, in *Scanning Tunneling Microscopy*, edited by J. A. Stroscio and W. J. Kaiser (Academic, San Diego, 1993).
[7] W. Han, E. R. Hunt, O. Pankratov, and R. F. Frindt, Phys. Rev. B **50**, 14 746 (1994).
[8] M. Tanaka, S. Yamazaki, K. Kajimura, H. Bando, T. Nakashizu, N. Morita, W. Mizutani, and M. Ono, J. Microsc. **152**, 183 (1988).
[9] M. Tanaka, H. Tokumoto, T. Nakashizu, W. Mizutani, K. Kajimura, S. Yamazaki, M. Ono, and H. Bando, Jpn. J. Appl. Phys. **28**, 473 (1989).
[10] B. Parkinson, J. Am. Chem. Soc. **112**, 7498 (1990).
[11] A. P. Volodin and J. Aarts, Physica C **235**, 1909 (1994).
[12] E. Delawski and B. A. Parkinson, J. Am. Chem. Soc. **114**, 1661 (1992).
[13] T. Hasegawa, W. Yamaguchi, J.-J. Kim, W. Wei, M. Nantoh, H. Ikuta, K. Kitazawa, A. Manivannan, A. Fujishima, and K. Uchinokura, Surf. Sci. **314**, 269 (1994).
[14] R. Manzke, T. Buslaps, B. Pfalzgraf, M. Skibowski, and O. Anderson, Europhys. Lett. **8**, 195 (1989).
[15] B. Dardel, M. Grioni, D. Malterre, P. Weibel, Y. Baer, and F. Levy, Phys. Rev. B **45**, 1462 (1992).
[16] J.-J. Kim, W. Yamaguchi, T. Hasegawa, and K. Kitazawa, Phys. Rev. Lett. **73**, 2103 (1994).
[17] W. J. Wattamaniuk, J. P. Tidman, and R. F. Frindt, Phys. Rev. Lett. **35**, 62 (1975).